energy&fuels

pubs.acs.org/EF

Article

Dimethyl Carbonate Synthesis via Transesterification of Propylene Carbonate Using a Titanium−Praseodymium-Based Catalyst

Surbhi Dahiya, Vimal Chandra Srivastava,* and Vimal Kumar

Cite This: *Energy Fuels* 2022, 36, 13148−13158

Read Online

ACCESS | Metrics & More | Article Recommendations | Supporting Information

ABSTRACT: Dimethyl carbonate (DMC) and propylene glycol (PG) synthesis through a methanol and propylene carbonate (PC) reaction, also referred to as a transesterification reaction, is a new and green alternative to other routes, such as phosgene methanolysis, urea methanolysis, etc. In this paper, the titanium−praseodymium-based catalyst prepared via the co-precipitation method has been used to improve the yield and selectivity of DMC production. Different combinations of catalysts were synthesized, referred to as $Ti_{0.99}Pr_{0.01}$, $Ti_{0.97}Pr_{0.03}$, $Ti_{0.96}Pr_{0.04}$, and $Ti_{0.95}Pr_{0.05}$, according to the molar ratio of Ti with respect to Pr. The catalysts have been studied and analyzed through various characterization techniques, such as X-ray diffraction (XRD), field emission scanning electron microscopy (FESEM), Fourier transform infrared spectroscopy (FTIR), and X-ray photoelectron spectroscopy (XPS). The Brunauer−Emmett−Teller (BET) surface area and pore volume diameter have been studied through N_2 adsorption−desorption using BET and Barrett−Joyner−Halenda (BJH) models, respectively. The basicity was determined through the carbon dioxide temperature-programmed desorption (CO_2-TPD) for understanding the reaction mechanism. The reaction was carried out in the batch reactor, keeping the temperature range of 160−180 °C and the molar ratio of methanol/PC in the range of 3−10. The study has also been made on oxygen vacancy concentrations in the mixed oxide catalysts as a result of the mixing of Pr with Ti, thereby affecting the yield and selectivity of DMC. The maximum yield of DMC was obtained with the $Ti_{0.96}Pr_{0.04}$ catalyst at a temperature of 170 °C which resulted in the PC conversion of 81.7%, turnover frequency (TOF) of 0.120 h^{-1}, and selectivity of 71.6% for DMC.

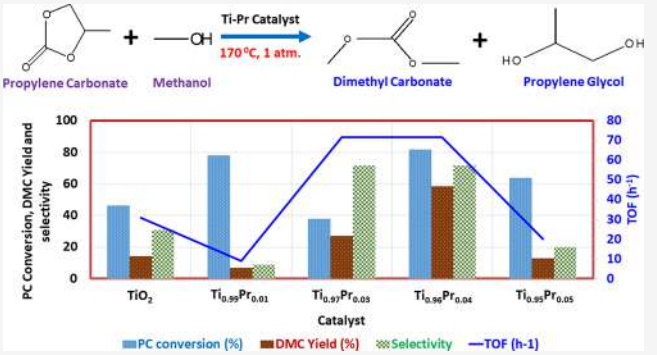

1. INTRODUCTION

The demand for fuels and additives has been traditionally fulfilled through the use of coal, natural gas, etc. However, these chemicals emit harmful gases in the atmosphere that make them environmentally unsustainable.[1] Hence, it is desirable to use green chemicals that help in combating these emissions and also provide an alternative to biodegradable substances.[2] One such chemical that is highly oxygenated with about 53 wt % oxygen content is dimethyl carbonate (DMC), which can be used in several industries, including fuel, cosmetics, paint, polymer, etc.[3] It is biodegradable in nature and can be used in lithium batteries as an additive.[4] It finds its applications as a raw material during carbonylation and methylation reactions and as an alternative to several toxic chemicals, such as methyl chloroformate, dimethyl sulfate, and phosgene, and can be used for the production of polyurethane, polycarbonate, etc.[5−8]

There are several routes through which DMC can be produced that include methanolysis of phosgene/urea, oxidative carbonylation of methanol,[7] electrochemical method, transesterification of methanol using propylene carbonate (PC)/ethylene carbonate (EC) with methanol, and direct synthesis from carbon dioxide and methanol.[8] The conventional route of phosgenation is now banned in several countries as a result of the toxicity of phosgene, the production of hazardous waste products, and its harmful effects on the environment. The green route is the direct synthesis route utilizing carbon dioxide that helps curb greenhouse gas emissions in the atmosphere and uses it to produce DMC. However, this route has a thermodynamic constraint because it is non-spontaneous and involves the production of water. The route that is currently used for the production of DMC is methanol oxycarbonylation; however, it suffers from various setbacks. In this process, Cu halide is used, which is a homogeneous catalyst; hence, the separation from the product becomes difficult.[9] To overcome these problems, in this paper, the study has been made on the transesterification route in which methanol and PC are used as raw materials, and the

Received: July 4, 2022
Revised: October 4, 2022
Published: October 21, 2022

Scheme 1. Transesterification Reaction of PC with Methanol[11]

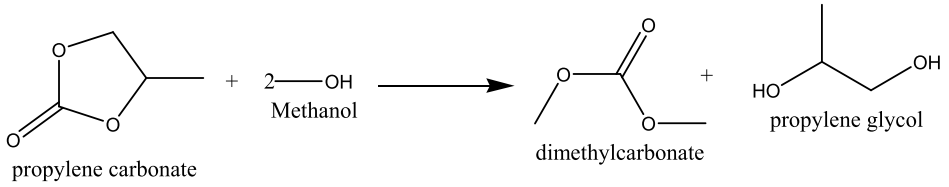

reaction can be carried out in the batch reactor in the presence of catalysts and produce the major products, DMC and propylene glycol (PG). The production of PG as a product in this reaction is also an advantage because it can also be used in the chemical industry after its separation from the products.[9]

Historically, various homogeneous catalysts were employed, but they pose a problem of separation from the product. Recently, heterogeneous catalysts have been adopted in the reaction that include bimetallic oxides, which resulted in increased PC conversion and an effective yield of DMC.[10] Kumar et al.[8] used Ce−M (M = Co, Fe, Cu, and Zn) for this reaction and found that maximum basicity was obtained with the combination of Ce−Cu and, hence, increased the DMC yield to 71.9%. The same group used the Ce−Zn catalyst with different chelating agents and achieved a DMC selectivity of 95%. Song et al.[11] used a Fe−Mn double metal cyanide catalyst and found DMC selectivity to 90.3%. Catalysts, such as alkali metals, KF-supported metals, zeolites, metal−organic frameworks, double-layered hydroxides, etc., have been employed for this route of reaction. Apart from metallic oxides, the employability of graphene-based catalysts in the reaction is a novel contribution to this field of research. Many chemical processes, including the preparation of DMC through transesterification, can be performed using N-functionalized graphene oxide, which is also a metal-free catalyst.[12] Kumar et al.[13] used nitrogen-functionalized graphene oxide nanosheets and obtained a DMC yield of nearly 50%. The use of double-layered catalysts reported by Liao et al.[14] achieved 96.3% DMC selectivity.

Praseodymium-based catalysts have been used for several reactions as a result of their unique properties.[15] Pu et al.[16] carried out the CO oxidation reaction of Pr over Cu-doped CeO_2 and found the enhanced activity as a result of the reason that the oxygen vacancy created because of doping provided activation centers for chemisorption for CO. Devaiah et al.[17] used ceria-mixed praseodymium for carrying out the CO oxidation as a result of its superior bulk oxygen mobility and its capability of forming dioxides because of the existence of +3 and +4 oxidation states.

The synthesis of $Ce_{0.8}M_{0.0.12}Sn_{0.08}O_{2-\delta}$ was used for CO oxidation, and it was found that this combination has led to a better oxidation capacity because Pr has led to a high surface area and superior surface oxygen vacancies.[18] Tang et al.[19] studied the first-principle investigation by doping CeO_2 with Pr for creating the oxygen vacancy in the lattice as a result of the half-filled orbitals present in the dopant Pr. Westermann et al.[20] studied the defect bands, which were enhanced as a result of the resonance Raman effect while doping CeO_2 with Pr that helped reduce Pr^{4+} cations, thereby modifying the electronic properties of the catalyst.

It is also evident from the literature that the basicity of catalysts is of utmost importance for the better achievement of yield and selectivity of DMC in this particular reaction.[17−21] The transesterification reaction of PC with methanol is shown in Scheme 1.[11]

In this paper, Pr was mixed with TiO_2, prepared through sonication, which means the mixing of rare-earth metals into titanium dioxide because rare-earth metals have separate electron configurations and are bound to form complexes with various groups, such as acids, amines, aldehydes, alcohols, etc., through the interaction of these functional groups with the f orbital of lanthanides.[22] This kind of interaction helps in the conversion of PC and improves the selectivity of DMC during the transesterification reaction because Pr has the ability in complexing PC through the interaction of their functional groups with the f orbital of lanthanides. Further, this combination enables the formation of an anatase form of TiO_2, which gives the metastable structure of the catalyst, well-meant for this reaction.[23] The prepared catalysts were characterized using X-ray diffraction (XRD), Brunauer−Emmett−Teller (BET), X-ray photoelectron spectroscopy (XPS), Fourier transform infrared spectroscopy (FTIR), and field emission scanning electron microscopy (FESEM), and the basicity of the catalysts was calculated using carbon dioxide temperature-programmed desorption (CO_2-TPD). A mechanistic scheme is being proposed in understanding the mechanism of adsorption of methanol on the surface of the catalyst and enabling the reaction to occur. The study has been made in a manner to find out the optimum conditions in terms of parameters such as the temperature, methanol/PC ratio, and catalyst dose in the reaction for enhancing DMC selectivity.

2. MATERIALS AND METHODS

The chemicals used in the reaction were of analytical reagent (AR) grade and were used without any refinement. The raw materials titanium oxide (TiO_2, 99%), praseodymium(III) nitrate hexahydrate [$Pr(NO_3)_3{\cdot}6H_2O$, 99.9%], PC ($C_4H_6O_3$, 99%), dimethyl carbonate ($C_3H_6O_3$, 99%), and methanol (CH_3OH) were bought from LOBA Chemie Pvt. Ltd. The water used during experiments was demineralized water, so that the quality of the end products remains intact.

2.1. Synthesis of Ti−Pr Metal Oxides with Different Molar Ratios. A series of Ti−Pr ($Ti_{100-x}Pr_xO_2$, where x = 0.01, 0.03, 0.04, and 0.05) catalysts were prepared by mixing TiO_2 and $Pr(NO_3)_3{\cdot}6H_2O$ through the sonication method.[24] In this process, TiO_2/PrO_2 catalysts with different molar ratios (Ti/Pr = 0.05, 0.04, 0.03, and 0.01) were prepared by mixing titanium(IV) oxide and praseodymium nitrate through sonicating in the sonicator.[25] At first, the appropriate amount of praseodymium salt (according to the molar ratio) was dissolved in 100 mL of demineralized water and sonicated for 30 min at 60 °C. After the sonication, the estimated amount of titanium oxide was dispersed and stirred (200 rpm) at room temperature for the next 30 min. Now, the solution was made to evaporate at 80 °C, keeping the stirring rate at 350 rpm. Further drying was made in air at 90 °C for the next 12 h. The materials were annealed in the furnace at 500 °C under airflow (40 cm^3/min) for 4 h with a 2 °C/min heating rate.

The synthesized catalysts were denoted as $Ti_{0.99}Pr_{0.01}$, $Ti_{0.97}Pr_{0.03}$, $Ti_{0.96}Pr_{0.04}$, and $Ti_{0.95}Pr_{0.05}$ for catalysts having Pr/Ti molar ratios of 0.01, 0.03, 0.04, and 0.05, respectively. The entire procedure of the

https://doi.org/10.1021/acs.energyfuels.2c02235
Energy Fuels 2022, 36, 13148−13158

preparation method helps in creating mesopores in the catalysts that helps in the adsorption process effectively.

2.2. Characterization. Powder XRD of the catalysts was performed using the Bruker D8 Advance diffractometer with Cu Kα radiation (λ = 1.5406 Å) having a step size of 0.02. The angle range considered was from 5° to 90°. The morphology of the catalysts was studied using FESEM using a Carl Zeiss Ultra Plus field emission electron microscope equipped with energy-dispersive X-ray spectroscopy (EDAX) operated at 16 kV.

Further, the textural properties of the catalysts were characterized using multipoint N_2 adsorption−desorption measurements at −195 °C using a Micromeritics ASAP 2020 apparatus. Before analysis, the catalysts were subjected to degassing at 200 °C under N_2 flow to remove any adsorbed impurities during this process. After degassing, the surface properties, such as surface area and pore volume diameter, were calculated through the BET and BJH models, respectively. The desorption branch of the isotherm helped in the calculation of the pore diameter and mean pore diameter using the Barrett−Joyner−Halenda (BJH) model. The total pore volume can be estimated by the amount adsorbed at P/P_0 = 0.99.

The basicity of the catalyst was determined using TPD of CO_2 on a Micromeritics Chemisorb 2720 apparatus fitted with a thermal conductivity detector (TCD). The process to determine the basicity includes placing the catalyst sample in a quartz U-tube and activating/pretreating at 200 °C under the flow of helium gas (20 cc/min) for approximately 6 h. Then, this sample was cooled to 50 °C and subjected to CO_2 adsorption by maintaining 10% CO_2/He flow of 20 cm^3/min to calculate the basicity. The desorption profile is further recorded in the range of 50−900 °C, keeping the heating rate at 10 °C/min under He flow (20 cm^3/min), and CO_2 was studied at TPD.

FTIR spectrophotometer (Thermo Nicolet, Model Magna 760) was used for the FTIR investigation of the catalysts. A KBr self-supported pellet technique was applied in studying the spectra in the range of 500−4000 cm^{-1}.

The catalyst activity of this reaction has been performed in the batch reactor of 50 mL. After the reaction, the product was analyzed using gas chromatography (GC, NETEL Micro-9100) equipped with a flame ionization detector (FID, 300 × 0.25 mm) column. GC was programmed at a temperature initially being 40 °C with the holding time of 10 min, and then the temperature was raised at the rate of 3 °C/min to 75 °C to reach 250 °C. Injector and detector temperatures were 250 and 260 °C, respectively.

2.3. Reaction Procedure. The prepared catalysts were tested for PC and methanol transesterification reaction in a batch reactor. The experiments were carried out in a 100 mL autoclave batch reactor. Initially, the appropriate amount of methanol, PC [keeping the required molar ratio (3−10)], and catalyst was kept in an autoclave in the different temperature range (160−170 °C), and the stirring rate varied between 500 and 650 rpm. The amount of catalyst used in the reaction is in the range of 2−6 wt % PC. Before the reaction occurs, the reactor is purged with N_2 and then an autogenic pressure is maintained. The reaction time was taken between 2 and 4 h. After the reaction, the product was cooled to 65 °C and then analyzed through GC. The samples to be used for the analysis at GC were prepared using biphenyl as an internal standard. Precisely, 800 μL of the reaction sample was mixed with 200 μL of biphenyl. Out of this, 1 μL of the sample was injected into GC in the split mode. The calculation of PC conversion and DMC yield was calculated through the following equations:

$$\text{PC conversion (\%)} = \frac{(\text{initial moles of PC} - \text{final moles of PC})}{\text{initial moles of PC}} \times 100 \quad (1)$$

$$\text{DMC yield} = \frac{\text{moles of DMC produced}}{\text{initial moles of PC}} \times 100 \quad (2)$$

3. RESULTS AND DISCUSSION

3.1. XRD Analysis. The XRD study of the $Ti_{100-x}Pr_xO_2$-type catalysts shows the presence of fluorite, cubic pyrochlore, monoclinic perovskite, tetragonal, etc.[26] In the XRD pattern of $Ti_xPr_{100-x}O_2$ (Figure S1a of the Supporting Information), the most intense peak can be found at a diffraction angle 2θ = 25.84°, indicating the presence of anatase (TiO_2),[27] with the tetragonal structure corresponding to the plane (011), which is a metastable structure very much suitable for the conversion of DMC. Along with anatase, the rutile phase (2θ = 54.34°) can also maintain the tetragonal structure. The weaker peaks at 38.31°, 55.29°, and 69.26° showed the exhibition of the cubic structure of β-titanium with planes (101), (002), and (112), respectively. The intensity of the peak decreased at 25.86° in the compound $Ti_{0.95}Pr_{0.05}O_2$ as a result of the increasing amount of praseodymium in the mixed oxide (Figure S1a of the Supporting Information). As the amount of praseodymium increased (from x = 0.01−0.04), the incorporation of praseodymium in the titanium species would have been uniform, with better dispersion of praseodymium species in the titanium lattice, which did not happen as the ratio was further increased to x = 0.05. As the ratio increased, there could have been a distortion in the structure of TiO_2 with the incorporation of PrO_2. The calculation of the average size of crystallite was performed using the Scherrer equation respective to the plane (011) (Table 1). The average size of the crystallite was calculated from the dominating peak of the anatase (011) plane, in which $Ti_{0.99}Pr_{0.01}$ and $Ti_{0.96}Pr_{0.04}$ exhibited a similar size of 43.1 nm. There is no dominating trend of increase or decrease of the crystalline size in the similar fashion of the prepared catalysts, maybe due to the formation of other phases of titanium, precisely rutile that is slightly merged with the anatase phase, confirming that the transition to the rutile phase is inhibited with the mixing of Pr in TiO_2.[22] The uneven patterns in the crystallite size may also be due to the segregation of Pr^{3+} at the grain boundary.

Table 1. Crystalline and Surface Properties of Catalysts

	plane (101)				
sample	2θ (deg)	d (nm)	crystalline size (nm)	BET surface area (m^2/g)	pore volume (g/cm^3)
$Ti_{0.99}Pr_{0.01}$	25.86	0.344	43.1	5.74	0.00100
$Ti_{0.97}Pr_{0.03}$	25.58	0.348	43.1	6.27	0.00047
$Ti_{0.96}Pr_{0.04}$	25.22	0.353	62.6	7.52	0.00033
$Ti_{0.95}Pr_{0.05}$	25.41	0.350	54.7	9.31	0.00067

3.2. Functional Group Analysis by FTIR and XPS. The FTIR spectra of the prepared catalysts were studied between 500 and 4500 cm^{-1} (Figure S1b of the Supporting Information). It was found that the peak near 3000−3500 cm^{-1} is attributed to the hydroxyl group that may be present in the catalyst. This hydroxyl group is conducive to the formation of DMC because oxygen vacancy can be created during the reaction that occurs at a high temperature. This means that the presence of the −OH group has the capability of creating O_v (oxygen vacancy) when the catalyst is participating in the transesterification reaction. The peaks near 1620 cm^{-1} were observed as a result of the mixing of Pr−TiO_2 and were similar for all prepared catalysts.[22] Further, there is a peak near 1570 cm^{-1} as a result of C═N bonding, mainly present in all prepared catalysts. There is a dip near 560 cm^{-1}, which

https://doi.org/10.1021/acs.energyfuels.2c02235
Energy Fuels 2022, 36, 13148−13158

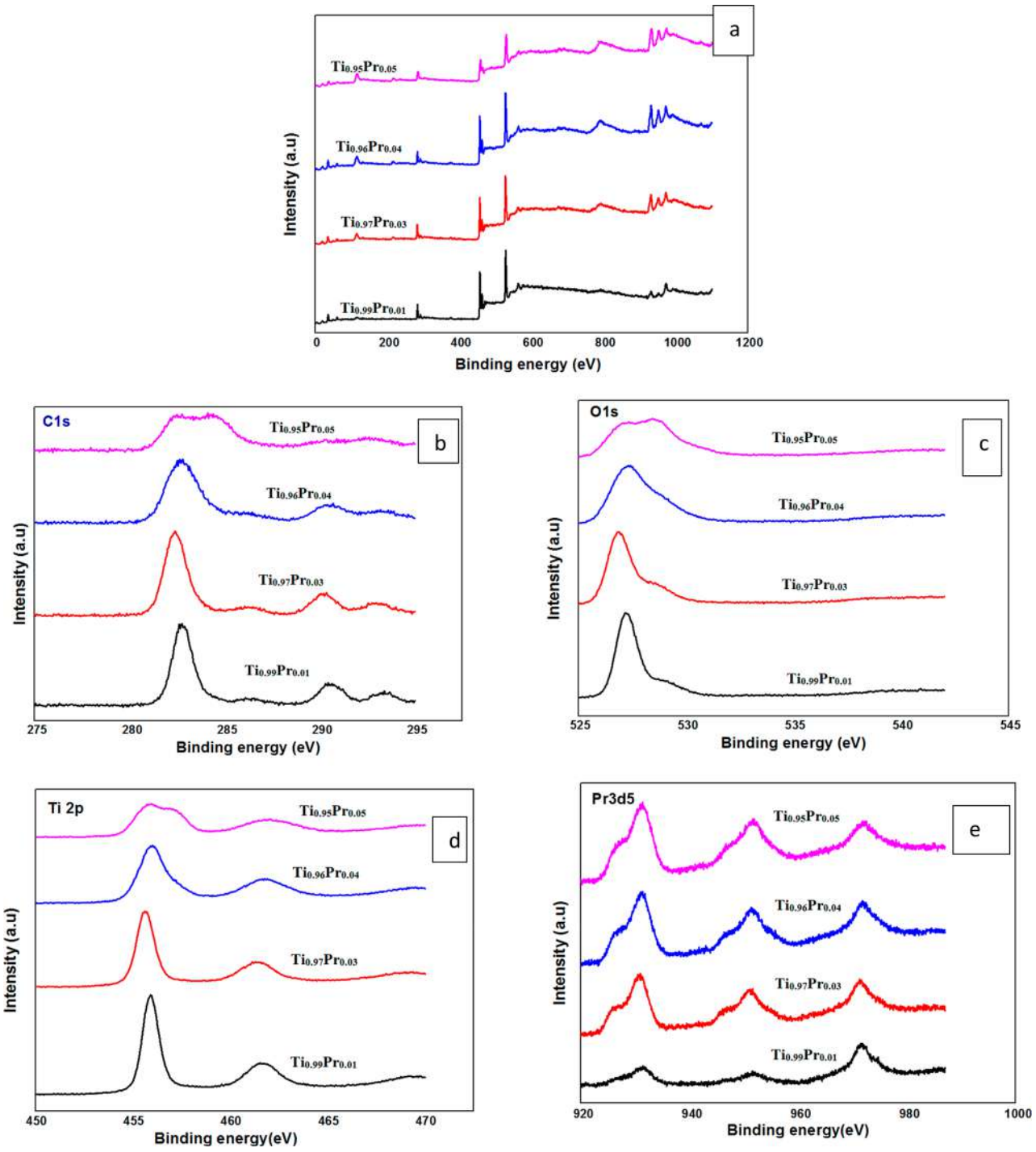

Figure 1. (a) XPS of the prepared catalysts $Ti_{0.99}Pr_{0.01}$, $Ti_{0.97}Pr_{0.03}$, $Ti_{0.96}Pr_{0.04}$, and $Ti_{0.95}Pr_{0.05}$, (b) C 1s of all of the catalysts, (c) O 1s of all of the prepared catalysts, (d) Ti 2p of all of the prepared catalysts, and (e) Pr 3d5 of all of the prepared catalysts.

corresponds to the formation of bonding of Ti in TiO_2 in the anatase form, leading to the stretching of Ti−O.[28]

The presence of various functional groups in the catalysts was found using the XPS technique (Figure 1a). This analysis of the prepared catalysts made through XPS helped determine the main elements present in the atomic percentage and the peaks of different orbitals. The peaks show four major elements in different states and orbitals, namely, C 1s, O 1s, Ti 2p, and Pr 3d5. The deconvoluted spectra of C 1s at around 284.78 eV reflects the presence of C═C (sp^2). The peak of carbon was due to the organic content that may be present as a result of the annealing of the catalyst. The binding energies of Ti $2p_{1/2}$ and Ti $2p_{3/2}$ were 464.58 and 456.5 eV, respectively.[29] This indicated that titanium mainly existed as Ti^{4+}. As per the literature, Ti $2p_{1/2}$ in pure TiO_2 appears at 459.05 eV; hence, the shift is attributed to the change in the mixing of Pr to the titanium, hence forming the bonds of Pr−O−Ti on the TiO_2 surface. There is a shift in the peak position of Ti 2p in the case of $Ti_{0.95}Pr_{0.05}$ toward 457 eV, representing intermediate Pr incorporation into TiO_2.[30] The O 1s peak that appears at 526.78 eV is the characteristic peak of lattice oxygen (Ti−O), and the shift of the peak in $Ti_{0.95}Pr_{0.05}$ toward 530 eV

https://doi.org/10.1021/acs.energyfuels.2c02235
Energy Fuels 2022, 36, 13148−13158

represented the Pr−O bond in the Pr_2O_3 form. There are dominantly two peaks corresponding to Pr 3d. The peak at 934.67 eV (Pr $3d_{5/2}$ (predominantly the state of Pr^{3+}) corresponds to the formation of Pr−O, and the peak at 952.2 eV corresponded to the formation of Pr−O−Ti. As it is known, the ionic radius of Pr^{3+} is larger than that of Ti^{4+}, which means that the Ti^{4+} ion could fit into the lattice of Pr^{3+}, thus changing the electron field and enhancing the activity of the reaction, enabling the moiety to enact.

3.3. Calculation of Surface Oxygen Vacancies and Identifying the Chemical States of the Catalysts. The XPS spectra of all of the prepared catalysts are shown in Figure 1a, through which different states of Pr whether present in Pr^{3+} or Pr^{4+} can be identified.[31] The above section has already discussed that the peak near 934.67 eV corresponds to the Pr^{3+} state, which shows that there is a creation of oxygen vacancy in the lattice. The peaks near 952.2 and 974.38 eV are related to the Pr^{4+} states. These bands will enable quantitative enumeration of the concentration of Pr^{3+} states by calculating through the equation:

$$C[Pr^{3+}] = \left(\frac{A_{Pr^{3+}}}{A_{Pr^{3+}} + A_{Pr^{4+}}}\right) \times 100 \quad (3)$$

The calculated percentage of Pr^{3+} to total Pr_{total} is 15.25, 21.58, 23, and 21.69% for TiPr(1), TiPr(2), TiPr(3), and TiPr(4), respectively. The oxygen vacancy that may be present on the surface of the catalysts is the potent site for the reaction and the formation of DMC through the transesterification routes. As the percentage of Pr in the lattice is increased, there is an enabling tendency of the presence of Pr^{3+} ions, thereby better oxygen vacancy. After the mixed oxide contained the Pr amount of more than 0.04 mol ratio, the Pr^{3+} concentration decreased as a result of the segregation of grains of Pr^{4+} in the lattice structure. This declining effect could be seen in the formation of DMC selectivity and yield also (Table 2). The O

Table 2. Catalyst Performance at 170 °C, Methanol/PC Ratio = 5, Catalyst Dose = 3 wt % PC, and Nitrogen Purging 8 bar at Autogenic Pressure

catalyst	PC conversion (%)	DMC yield (%)	TOF (h^{-1})	selectivity	PG/DMC
$Ti_{0.99}Pr_{0.01}$	77.9	6.948	0.115	8.9	3.500
$Ti_{0.97}Pr_{0.03}$	37.8	27.050	0.056	71.6	0.827
$Ti_{0.96}Pr_{0.04}$	81.7	58.447	0.120	71.6	0.071
$Ti_{0.95}Pr_{0.05}$	63.8	12.817	0.094	20.1	0.752

1s spectra of the catalysts determine that mainly two types of peaks can be seen: one near 526.78 eV and the other near 528.27 eV. The peak near 526.27 eV determines lattice oxygen O_L, and the peak near 528.78 eV determines the O^{2-} (O_v) ions present in surface oxygen vacancies.

The concentration of surface oxygen vacancies may be calculated through the following formula:

$$C[O_v] = \left(\frac{A_{O_v}}{A_{O_v} + A_{O_L}}\right) \times 100 \quad (4)$$

It has been found that the concentration of oxygen vacancies varied as 80, 82, 86, and 82% for $Ti_{0.99}Pr_{0.01}$, $Ti_{0.97}Pr_{0.03}$, $Ti_{0.96}Pr_{0.04}$, and $Ti_{0.95}Pr_{0.05}$, respectively. Mixing of Pr into Ti enabled the formation of surface oxygen defects/vacancies until the ratio of 0.04 mole fraction of Pr into the mixed oxides. After this, there occurs the sintering of the lattice structure with more Pr^{4+} ions.

3.4. Morphological Analysis. The morphology of the catalysts has been studied through FESEM (Figure 2). The images showed the mixing of praseodymium particles in titanium dioxide, and the particle size is within the range of 100 nm of sphere-like entities. The structure shows formation of nanoagglomerates that depict the mixing of Pr^{3+} in the Ti^{4+} lattice depicting the stable structure of the mixed oxides.[32] This is well in cognizance of the XRD data that showed that the particle size is in the nano range within 100 nm for all of the catalysts. TiO_2 mixed with Pr showed a uniform spherical structure with a nanosized particle diameter. As the amount of Pr increased in the mixed oxide, at first, there could be any significant change in the morphology of the catalysts, but after the mole fraction of Pr increased to 0.04, there occurred a larger conglomeration of particles, which inhibited the proper fitting of Pr^{3+} and Ti^{4+} in the mixed oxide (Figure 2).

3.5. Surface Analysis and TPD Analysis. The surface area and mesoporous structure of the catalysts were studied through N_2 adsorption and desorption isotherms (shown in Figure S2 of the Supporting Information and Table 1). The surface area increased as the content of Pr increased in the catalysts that enabled the better adsorption of species on the surface and the formation of methoxy ions. These methoxy ions then help increase the selectivity toward the formation of DMC. The desorption peak in the relative pressure range of 0.75−0.96 establishes the hysteresis curve H_2 (Figure S2 of the Supporting Information), showing mesopore formation in the prepared catalysts. This type of mesopore is an added advantage for the transesterification reaction.

To calculate the basicity in the catalyst, CO_2-TPD (Figure S3 of the Supporting Information) was performed for all of the catalysts and analyzed through TCD signals obtained at different temperatures. The peaks are divided between low and moderate basic sites and strong basic sites by studying their behavior within different temperature ranges.[8] Within the domain of 200 °C, there exist moderate basic sites and strong basic sites for temperatures ranging from 400 and 600 °C and super basic sites beyond 600 °C. The introduction of Pr in the catalyst led to the formation of super strong basic sites, giving a DMC selectivity of 71.6% and a high PC conversion (Table 2).

For the catalyst $Ti_{0.99}Pr_{0.01}$, the major peaks were found at 321, 416, and 620 °C, whereas for $Ti_{0.97}Pr_{0.03}$, the peaks were found near 142, 340, and 640 °C. For $Ti_{0.96}Pr_{0.04}$, there are four peaks found near 109, 344, 593, and 820 °C. There is no dominant peak found for $Ti_{0.95}Pr_{0.05}$ in the super strong region. This brings into reasoning that the basic sites, especially the super strong sites, are responsible for the better DMC yield and selectivity.[33] The calculated basicity for $Ti_{0.99}Pr_{0.01}$, $Ti_{0.97}Pr_{0.03}$, and $Ti_{0.96}Pr_{0.04}$ was 0.0077, 0.01088, and 0.0147 mmol/g, respectively.

3.6. Reaction and Catalyst Performance. The catalytic activity for all of the prepared catalysts, i.e., $Ti_{0.99}Pr_{0.01}$, $Ti_{0.97}Pr_{0.03}$, $Ti_{0.96}Pr_{0.04}$, and $Ti_{0.95}Pr_{0.05}$, was tested for the transesterification of methanol and PC to form DMC and PG in the batch reactor (Figure 3 and Table 2). The results in Table 2 give the PC conversion, turnover frequency (TOF), and DMC yield and selectivity. The calculated TOF values for the catalysts $Ti_{0.99}Pr_{0.01}$, $Ti_{0.97}Pr_{0.03}$, $Ti_{0.96}Pr_{0.04}$, and $Ti_{0.95}Pr_{0.05}$ were 0.115, 0.056, 0.120, and 0.094, respectively. The comparison has been made using pure TiO_2 as the catalyst

https://doi.org/10.1021/acs.energyfuels.2c02235
Energy Fuels 2022, 36, 13148−13158

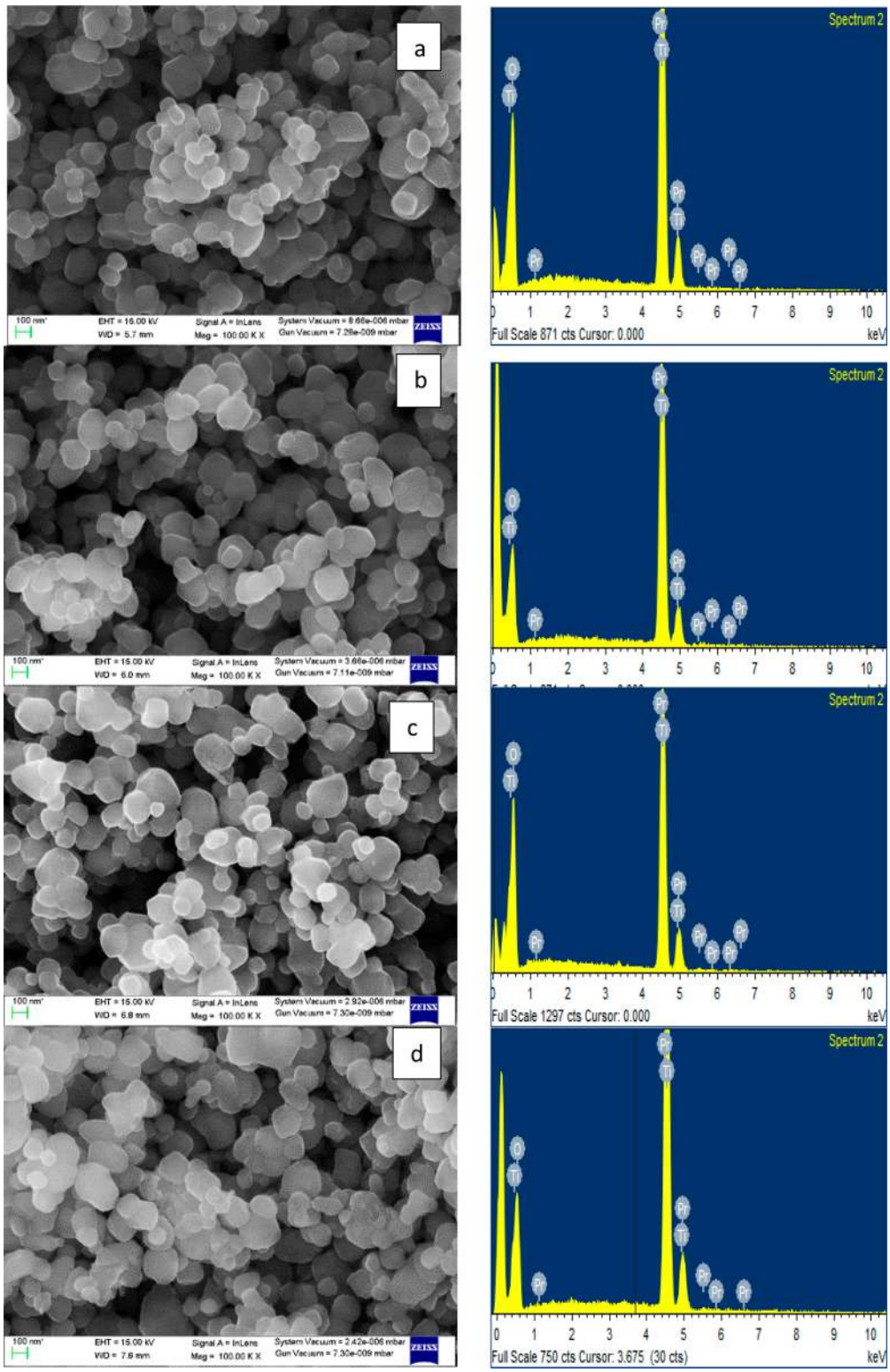

Figure 2. FESEM images of the prepared catalyst: (a) $Ti_{0.99}Pr_{0.01}$, (b) $Ti_{0.97}Pr_{0.03}$, (c) $Ti_{0.96}Pr_{0.04}$, and (d) $Ti_{0.95}Pr_{0.05}$.

for the same reaction. It has been found that PC conversion was as low as 46.34% and yield of 14.39% when pure TiO_2 was used as the catalyst (Figure 3). This reflected that addition of Pr to TiO_2 has enhanced the PC conversion, yield, and selectivity during the reaction.

Further, the catalyst activity was determined by calculating the basic sites for all of the catalysts. The maximum activity was found for $Ti_{0.96}Pr_{0.04}$. BET analysis showed that the presence of mesopores has an impact on the better performance of the catalysts. The surface area increased as the Pr amount increased in the catalysts; however, the low performance for $Ti_{0.95}Pr_{0.05}$, even though it has a high surface area, maybe due to the sintering of Pr particles into the mixed oxide catalysts, which further weakened the selectivity toward DMC. The oxygen vacancy concentrations increased with the increase of Pr in Ti (up to the molar ratio of 0.04 of Pr), which

https://doi.org/10.1021/acs.energyfuels.2c02235
Energy Fuels 2022, 36, 13148−13158

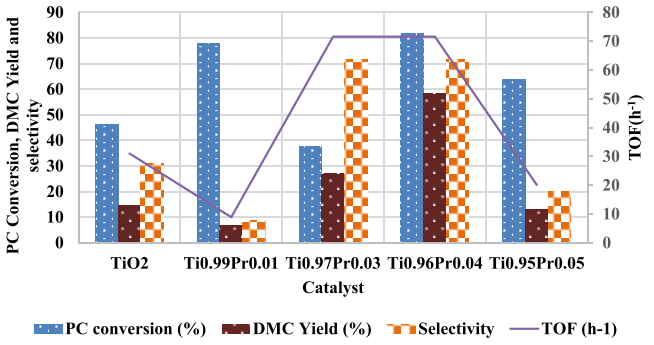

Figure 3. PC conversion, DMC yield, and selectivity at optimum conditions of temperature = 170 °C, methanol/PC ratio = 5, catalyst dose = 3.5 wt % PC, and stirring speed = 600−650 rpm.

affected the yield and selectivity of DMC in the reaction. The defects/vacancies created lead to the adsorption of methanol on the surface of the catalyst, thereby forming methoxy ion and H^+ ion. This leads to the shift of equilibrium toward DMC production.

3.6.1. Catalyst Dose. The catalyst, $Ti_{0.96}Pr_{0.04}$, dose was varied from 2 to 6 wt % PC to determine the effect of catalyst on the reaction in terms of DMC yield and selectivity (Figure 4a). It has been found that, with the catalyst dose of 2 wt % PC, the PC conversion was 46.7%, whereas the DMC yield and selectivity were 18.4 and 39.4%, respectively. In comparison, the PC conversion, DMC yield, and selectivity all increased when the catalyst dose was increased to 3.5 wt % PC. This is due to the increased surface area and the availability of the active sites for the reaction with the increase in the catalyst dose. The PC catalyst dose of 6 wt % increased the PC conversion to 86.26%, but the DMC yield and selectivity decreased to 7.48 and 8.6%, respectively. This may be due to the deviation of the reaction toward the formation of PG. The decreased DMC yield may be ascribed to the poor dispersion of the catalyst at higher doses. The excess of catalyst mass can lead to inhibition of the charge transfer reaction at the catalyst surface, thereby decreasing the DMC yield. Hence, the most optimum catalyst dose for this reaction obtained was 3.5 wt % PC.

3.6.2. Reaction Time. The reaction has been studied for the optimum catalyst $Ti_{0.96}Pr_{0.04}$ by varying the reaction time (Figure 4b). The initial reaction has been carried out in a batch reactor for 2 h and subsequently increased the time to 4 and 6 h. When the reaction was carried for 2 h, the PC conversion was 77.24%, whereas the DMC yield and selectivity were 18.9 and 24.5%, respectively. This may be due to the less exposure time for the intermediate formed 2-methyl-hydroxyethyl methyl carbonate (2-HMC, shown in later in the mechanism) to convert to DMC. The maximum yield and selectivity for the reaction occurred at a 4 h time period in which the PC conversion was 81.7% and DMC yield and selectivity were 58.4 and 71.6%, respectively. Kumar et al.[17] showed that 6 h was the optimum condition for this reaction, and any further increase did not lead to a further effect on the reaction. For $Ti_{0.96}Pr_{0.04}$,

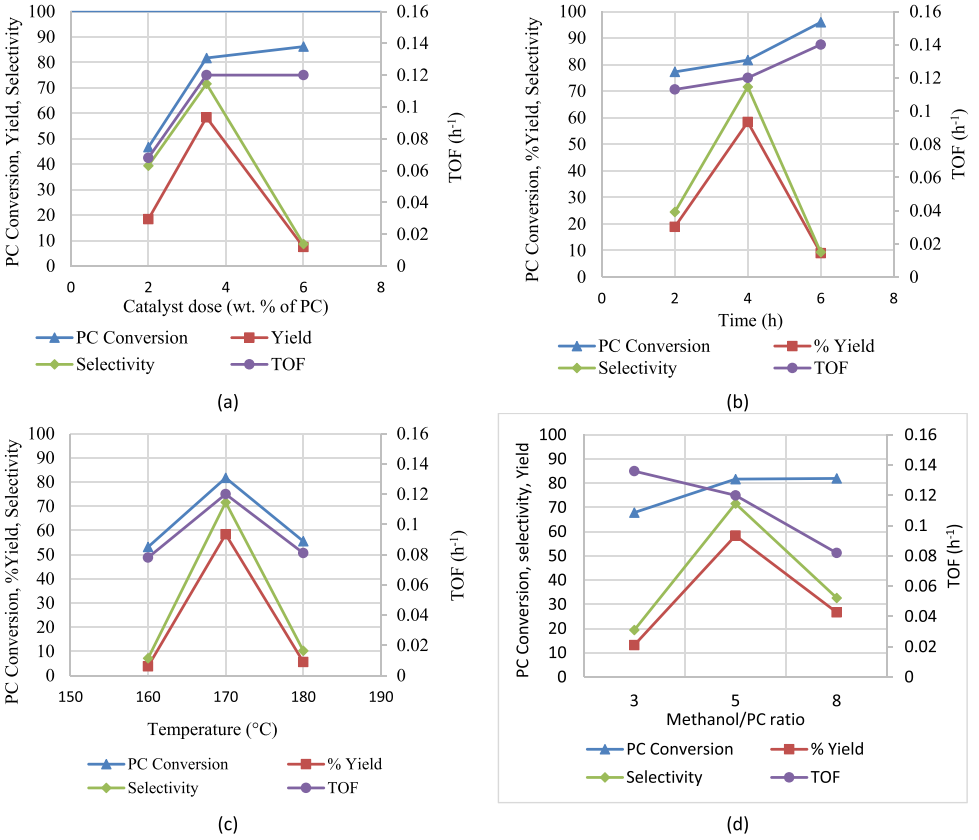

Figure 4. Graphical representation of the effect of operating parameters on PC conversion, DMC yield, selectivity, and TOF using the $Ti_{0.96}Pr_{0.04}$ catalyst. (a) Catalyst dose (2−6 wt % PC), time = 4 h, temperature = 170 °C, and methanol/PC = 5:1, (b) time (2−6 h), catalyst dose = 3.5 wt % PC, temperature = 170 °C, and methanol/PC ratio = 5:1, (c) temperature (160−180 °C), time = 4 h, catalyst dose = 3.5 wt % PC, and methanol/PC ratio = 5:1, and (d) methanol/PC ratio (3:1−8:1), time = 4 h, temperature = 170 °C, and catalyst dose = 3 wt % PC.

https://doi.org/10.1021/acs.energyfuels.2c02235
Energy Fuels 2022, 36, 13148−13158

with the further increase in the reaction time to 6 h, the PC conversion increased to 95.9%. However, the reaction favored the formation of PG, and the DMC yield and selectivity decreased to 9.0 and 9.39%, respectively. This may occur as a result of the longer time provided to the reaction that increased the PC conversion first to 2-HMC and further to PG rather than DMC.

3.6.3. Reaction Temperature. The experiments for the most optimum catalyst $Ti_{0.96}Pr_{0.04}$ were performed at different temperatures to find out the effect of the temperature on the DMC yield and selectivity (Figure 4c). The other parameters, such as the initial purging pressure of N_2, catalyst dose, methanol/PC ratio, and time of the reaction, were kept constant. At 160 °C temperature, it was found that the PC conversion was 53.15%, whereas the DMC yield and selectivity were very low, precisely 3.7 and 7.13%, respectively. With the increase of the temperature to 170 °C, the PC conversion, DMC yield, and selectivity increased to 81.7, 58.4, and 71.6%, respectively. This is due to the higher kinetic energy possessed by the reactant molecules, enabling them to cross the activation barrier to yield the product. Further, an increase in temperature to 180 °C decreased the PC conversion, DMC yield, and selectivity to 55.4, 5.6, and 10.25%, respectively. The increase of the temperature from a certain value to 180 °C favored other side reactions, leading to the low selectivity and yield of DMC.[8] Wang et al.[34] reported 160 °C as the optimum condition for the highest yield and selectivity of DMC, but for the Ti−Pr catalyst, this temperature is 170 °C, which is also reported by Kumar et al.[8] and Devaiah et al.[17] with nitrogen-functionalized graphene oxide. This may lead to the formation of intermediate 2-HMC in a high amount, leading to an unfavorable temperature for DMC formation.

3.6.4. Methanol/PC Ratio. The methanol/PC ratio is crucial to understand because it helps determine whether the amount of methanol/PC should be increased or decreased to maximize the formation of DMC (Figure 4d). With the ratio of 3:1, the PC conversion was 67.9%, whereas the DMC yield and selectivity were very low, 13.2 and 19.4%, respectively. Hence, the ratio was increased to 5:1 where the PC conversion was 81.7% and DMC yield and selectivity were 58.44 and 71.6%, respectively. However, a further increase in the methanol/PC ratio to 8:1 led to the PC conversion of 82%, whereas the DMC yield and selectivity decreased to 26.7 and 32.6%, respectively. Different literature has reported 10:1 as the most optimum condition for the highest DMC yield for various sets of catalysts. Kumar et al.[8] have reported it to be 10:1 using Mg−Al hydrotalcite catalysts. PG and intermediate formation are more favored toward this condition (by increasing the methanol/PC ratio beyond 5:1 for this work). Therefore, according to the reaction, with a 5:1 methanol/PC conversion, the best conversion and DMC yield and selectivity were found.

3.6.5. Reusability of the Catalyst. The catalyst $Ti_{0.96}Pr_{0.04}$ was also tested for its efficiency and reusability in terms of the number of times it can be used for the reaction (Figure 5). After the use, it is centrifuged and reproduced by drying it in the oven at 70 °C for around 12 h. After drying, it is again used in the reaction at optimum conditions for PC conversion, DMC yield, and selectivity. The reaction was carried out at 170 °C, methanol/PC ratio of 5:1, and time of 4 h. The fresh catalyst resulted in the PC conversion of 81.7% and DMC yield and selectivity of 58.4 and 71.6%, respectively. After the first cycle, it is reproduced to understand how the catalyst performs in the transesterification reaction at the optimum

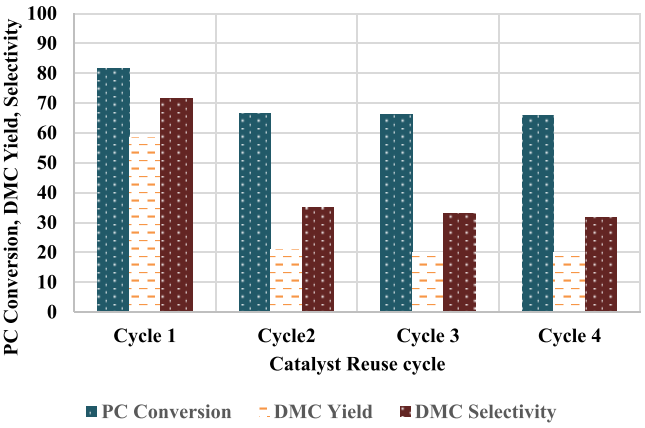

Figure 5. Reuse of catalyst $Ti_{0.96}Pr_{0.04}$ at optimum conditions (temperature = 170 °C, methanol/PC ratio = 5, catalyst dose = 3.5 wt % PC, and stirring speed = 600−650 rpm).

conditions. It is found that, in the second cycle of reuse, the PC conversion fell to 66.6% and DMC yield and selectivity fell to 20.8 and 35%, respectively. This reflected that DMC yield and selectivity decreased substantially as a result of sintering of catalyst sites and also difficulty in regaining the same amount of catalyst in the desired amount. After the third cycle, the PC conversion remained 66%, but DMC yield and selectivity reached 20 and nearly 30%, respectively. Hence, the catalyst may be reused for 4 cycles; after that, the performance of the catalyst decreases. This may have occurred as a result of the segregation of reactant molecules on the active sites.[17]

3.6.6. Reaction Kinetics and Mechanism. For the kinetic analysis, the effect of both PC and methanol has been considered. It is assumed that the reaction is first-order with respect to the concentration of both methanol (C_a) and PC (C_c).[35] Using the stoichiometry of the reaction, the concentration of methanol at time t is given as $C_a = C_{ao} - 2(C_{co} - C_c)$. Here, C_{ao} is the initial concentration of methanol, C_{co} is the initial concentration of PC, and C_c is the concentration of PC at time t. Assuming C_{ce} is the equilibrium concentration of PC, C_{ae} is the equilibrium concentration of methanol, t is the running time, and k is the kinetic constant, with the condition that $C_{ao} \gg 2(C_{co} - C_c)$, then the kinetic equation can be rewritten as[35]

$$\ln((C_{co} - C_{ce})/(C_c - C_{ce})) = kt \quad (5)$$

The above equation is the pseudo-first-order kinetic equation, where the rate-determining step depends only upon the concentration of PC only. The values of the rate constant (k), as calculated using the kinetic data (given in Figure 6a), were found to be 0.010 min^{-1} at 140 °C, 0.012 min^{-1} at 150 °C, 0.015 min^{-1} at 160 °C, and 0.021 min^{-1} at 170 °C. The activation energy as calculated from the Arrhenius plot (Figure 6b) was found to be 34.5 kJ mol^{-1}.

The mechanism can be enumerated in the schematic diagram given below (Figure 7). First, the basic sites on the catalyst activate methanol to produce the methoxy group, which means CH_3O^- and H^+ ions, in the reaction mixture. The anion formed becomes attached to carbonyl carbon of PC, forming an intermediate that absorbs H^+, which was formed in the previous step. This ion produces 2-HMC as the intermediate. This intermediate reacts with another methoxy ion and H^+ to produce DMC and PG.

https://doi.org/10.1021/acs.energyfuels.2c02235
Energy Fuels 2022, 36, 13148−13158

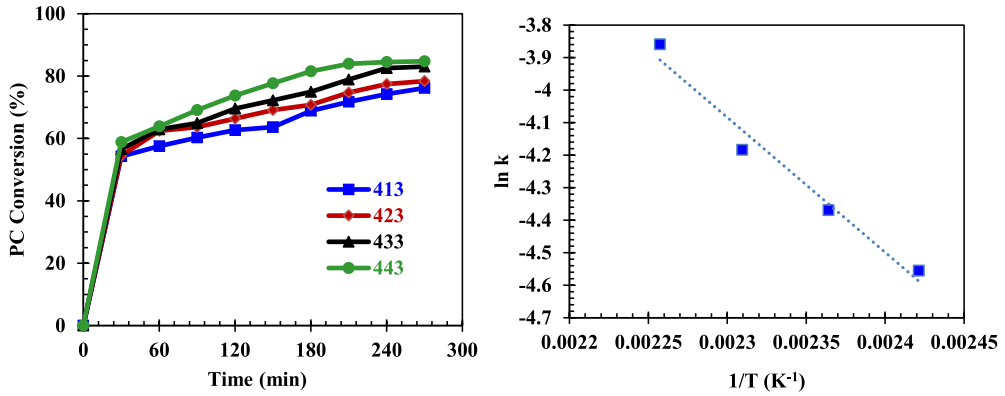

Figure 6. (a) Effect of the temperature on the PC conversion during the DMC synthesis reaction with the TiPr catalyst and (b) Arrhenius plot.

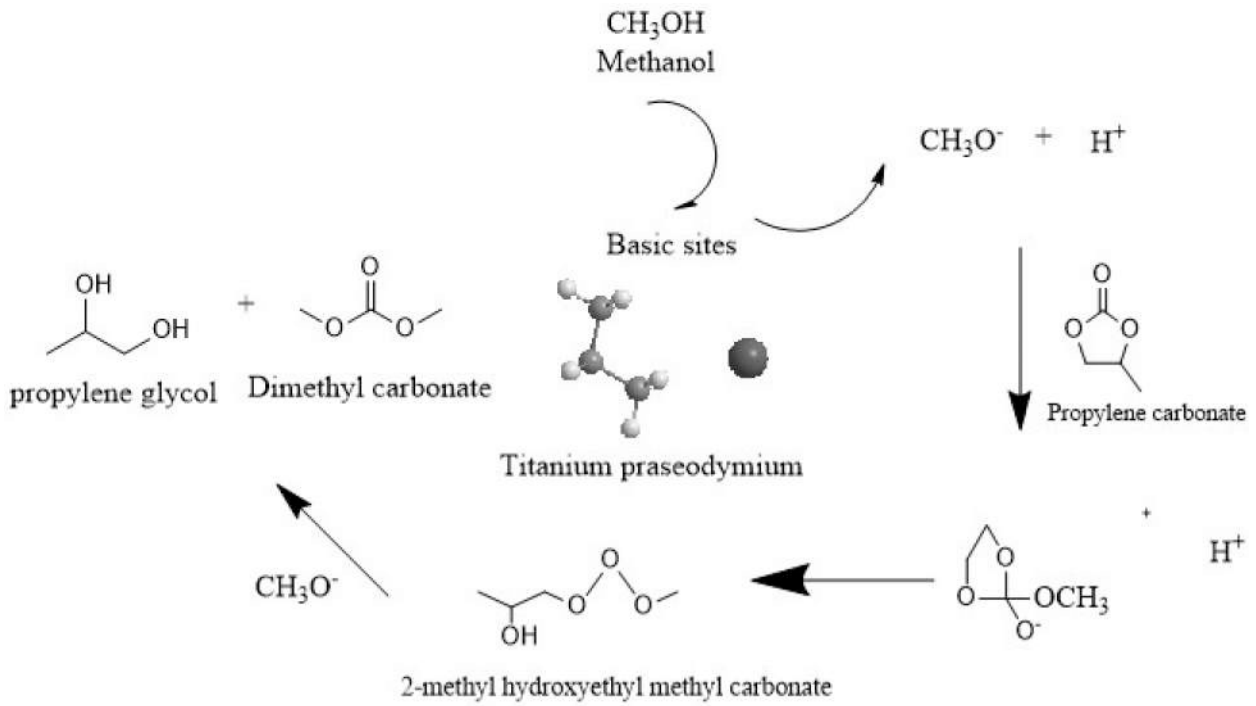

Figure 7. Schematic representation of transesterification of methanol and PC in the formation of DMC and PG in the presence of $Ti_{0.96}Pr_{0.04}$.

Table 3. Comparison of Different Catalysts in Terms of PC Conversion and DMC Yield

	operating conditions			performance				
catalyst	temperature (°C)	methanol/PC ratio	time (h)	catalyst dose (wt % PC)	yield (%)	selectivity (%)	PC conversion (%)	reference
Ca−M−Al						96.3		3
Ce−M(M = Co, Fe, Cu, and Zn)	160		4	5	71.9		65.4	8
CeO_2−La_2O_3 oxides	160					74−81	55−60	9
nitrogen-functionalized graphene oxide sheets	180		6	1	50			12
reduced graphene oxide with ZnO catalyst	180	2−10	4	3	74			13
ion-exchange resins	20−40	4−8				100		36
Ce−La oxides	140−180	4−12	2−10	2−10	74		72	37
Mg−Al solid base	65	10	4	4				38
Ti−Pr catalyst	165	5	4	3.5		71.6	81.7	this work

3.6.7. Comparative Assessment of the Catalytic Activity. Pyrlik et al.[36] carried out the transesterification process using ion-exchange resins as the heterogeneous catalyst. The pressure was autogenic, whereas other parameters, such as the molar ratio of methanol/PC, were varied in the range of 4−8, achieving selectivity close to 100%. Kumar et al.[37] used Ce−La oxides in different ratios for the transesterification reaction. The reaction was studied at different operating

https://doi.org/10.1021/acs.energyfuels.2c02235
Energy Fuels 2022, 36, 13148−13158

conditions, such as the methanol/PC ratio (4−12), catalyst dose (2−10 wt % PC), reaction time (2−10 h), and temperature (140−180 °C). The $Ce_{0.2}La_{0.8}$ catalyst gave the maximum DMC yield and PC conversion of 74 and 72%, respectively. Liao et al.[14] used solid base catalysts derived from Ca−M−Al (M = Mg, La, Ce, and Y) layered double hydroxides. The best catalytic performance obtained was of Ca−Mg−Al, which was also consistent with the basicity and total surface basic amounts and formation of strong basic sites for Mg. Along with basic surface sites, the unsaturated O^{2-} ions have also played an important part for enhanced catalytic activity. The maximum DMC selectivity obtained was 96.3% with catalyst Ce−Mg−Al. Table 3 compares the performance of the catalysts at varied conditions for the DMC synthesis reaction via transesterification of PC. Selectivity obtained in the present study was 71.6%. Some studies have reported better selectivity;[1436] however, many studies have reported lower selectivity as well.[1337] In the present work, TiPr was used as a catalyst. In comparison to other catalysts used in other literature, the optimum dosage of catalyst used was much lower compared to that reported in the literature. Pr mixing in the catalyst has been effective in improving the basicity of the reaction, thereby enhancing PC conversion.

4. CONCLUSION

The catalyst behavior at optimum conditions of 4 h, 165 °C (temperature), and 600−650 rpm (stirring speed) showed that the $Ti_{0.96}Pr_{0.04}$ catalyst gave the best conversion, yield, and selectivity as a result of the presence of basic sites on its surface, which became a favorable condition for creating oxygen vacancy on its surface, leading to greater selectivity for DMC. As the amount of Pr is increased beyond this limit, the conglomeration of Pr in TiO_2 hinders the selectivity of DMC and the formation of PG is favored more. Hence, $Ti_{0.96}Pr_{0.04}$ gives the best results in terms of the selectivity of DMC and PC conversion. The analysis made through the characterization of catalysts reflects that various properties, such as the nanosize of the catalyst, spherical morphology, strong basic sites, average surface area, and presence of the dominant anatase phase, are established in the $Ti_{0.96}Pr_{0.04}$ catalyst, which effectively improves the DMC yield and selectivity. The reaction of transesterification to produce DMC becomes viable and technically feasible through the use of a Ti−Pr set of catalysts when carried out in the batch reactor. The enhanced study made through various characterization techniques showed that the reaction requires a good amount of moderate and strong basic sites and appropriate oxygen vacancy on the surface of catalysts to enhance yield and selectivity of DMC in the transesterification reaction of methanol and PC to DMC and PG. The comparison between different catalysts used for this reaction has been enumerated in Table 3, which reflects that this work shows maximum PC conversion.

It is also studied that PC conversion may be high in many reaction cases, but selectivity toward DMC may not be large as a result of the deviation of the reaction toward the production of PG. The $Ti_{0.96}Pr_{0.04}$ catalyst possesses a good amount of basic sites with functional groups studied through FTIR and XPS to form suitable bonding with methanol and PC on its sites (for adsorption) for enhancing the selectivity of DMC toward 71.6%.

ASSOCIATED CONTENT

Supporting Information

The Supporting Information is available free of charge at https://pubs.acs.org/doi/10.1021/acs.energyfuels.2c02235.

XRD and FTIR (Figure S1), liquid nitrogen adsorption−desorption isotherm (Figure S2), and CO_2-TPD of the prepared catalysts (Figure S3) (PDF)

AUTHOR INFORMATION

Corresponding Author

Vimal Chandra Srivastava − *Department of Chemical Engineering, Indian Institute of Technology Roorkee, Roorkee, Uttrakhand 247667, India;* orcid.org/0000-0001-5321-7981; Phone: +91-1332-285889; Email: vimalcsr@yahoo.co.in, vimal.srivastava@ch.iitr.ac.in; Fax: +91-1332-27635

Authors

Surbhi Dahiya − *Department of Chemical Engineering, Indian Institute of Technology Roorkee, Roorkee, Uttrakhand 247667, India*

Vimal Kumar − *Department of Chemical Engineering, Indian Institute of Technology Roorkee, Roorkee, Uttrakhand 247667, India;* orcid.org/0000-0002-2140-7454

Complete contact information is available at: https://pubs.acs.org/10.1021/acs.energyfuels.2c02235

Notes

The authors declare no competing financial interest.

ACKNOWLEDGMENTS

The authors are thankful to the Science and Engineering Research Board, Department of Science & Technology, Government of India, New Delhi, India, for providing financial help for carrying out this research work under the Project EMR/2016/007510.

REFERENCES

(1) Chiang, C. L.; Lin, K. S.; Yu, S. H. Improvement of dimethyl carbonate formation via methanol carbonation over vanadium-doped Cu-Ni/AC catalysts. *J. Taiwan Inst. Chem. Eng.* **2019**, *98*, 132−149.

(2) Deng, W.; Shi, L.; Yao, J.; Zhang, Z. A review on transesterification of propylene carbonate and methanol for dimethyl carbonate synthesis. *Carbon Resour. Convers.* **2019**, *2*, 198−212.

(3) Liao, Y.; Li, F.; Pu, Y.; Wang, F.; Dai, X.; Zhao, N.; Xiao, F. Solid base catalysts derived from Ca−Al−X (X = F^-, Cl^- and Br^-) layered double hydroxides for methanolysis of propylene carbonate. *RSC Adv.* **2018**, *8*, 785−791.

(4) Wang, J.-Q.; Sun, J.; Cheng, W.-G.; Shi, C.-Y.; Dong, K.; Zhang, X.-P.; Zhang, S.-J. Synthesis of dimethyl carbonate catalyzed by carboxylic functionalized imidazolium salt via transesterification reaction. *Catal. Sci. Technol.* **2012**, *2*, 600−605.

(5) Pacheco, M. A.; Marshall, C. L. Review of dimethyl carbonate (DMC) manufacture and its characteristics as a fuel additive. *Energy Fuels* **1997**, *11*, 2−29.

(6) Tundo, P.; Selva, M. The chemistry of dimethyl carbonate. *Acc. Chem. Res.* **2002**, *35*, 706−716.

(7) Keller, N.; Rebmann, G.; Keller, V. Catalysts, mechanisms, and industrial processes for the dimethyl carbonate synthesis. *J. Mol. Catal. A: Chem.* **2010**, *317*, 1−18.

(8) Kumar, P.; Srivastava, V. C.; Mishra, I. M. Dimethyl carbonate synthesis by transesterification of propylene carbonate with methanol: Comparative assessment of Ce-M (M= Co, Fe, Cu and Zn) catalysts. *Renewable Energy* **2016**, *88*, 457−464.

(9) Cutrufello, M. G.; Atzori, L.; Meloni, D.; Piras, A.; Gazzoli, D.; Rombi, E. Synthesis of dimethyl carbonate by transesterification of propylene carbonate with methanol on CeO_2-La_2O_3 oxides prepared by the soft template method. *Materials* **2021**, *14*, 4802.
(10) Abimanyu, H.; Kim, C. S.; Ahn, B. S.; Yoo, K. S. Synthesis of dimethyl carbonate by transesterification with various MgO−CeO_2 mixed oxide catalysts. *Catal. Lett.* **2007**, *118*, 30−35.
(11) Song, Z.; Subramaniam, B.; Chaudhari, R. V. Transesterification of propylene carbonate with methanol using Fe-Mn double metal cyanide catalyst. *ACS Sustainable Chem. Eng.* **2019**, *7*, 5698−5710.
(12) Kumar, N.; Srivastava, V. C. Dimethyl carbonate production via transesterification reaction using nitrogen functionalized graphene oxide nanosheets. *Renewable Energy* **2021**, *175*, 1−13.
(13) Kumar, N.; Srivastava, V. C. Dimethyl carbonate synthesis via transesterification of propylene carbonate using an efficient reduced graphene oxide-supported ZnO nano catalyst. *Energy Fuels* **2020**, *34*, 7455−7464.
(14) Liao, Y.; Li, F.; Dai, X.; Zhao, N.; Xiao, F. Solid base catalysts derived from Ca-M-Al (M = Mg, La, Ce,Y) layered double hydroxides for dimethyl carbonate synthesis by transesterification of methanol with propylene carbonate. *Chin. J. Catal.* **2017**, *38* (11), 1860−1869.
(15) Stoian, D.; Medina, F.; Urakawa, A. Improving the stability of CeO_2 catalyst by rare earth metal promotion and molecular insights in the dimethyl carbonate synthesis from CO_2 with 2-cyanopyridine. *ACS Catal.* **2018**, *8*, 3181−3193.
(16) Pu, Z. Y.; Liu, X. S.; Jia, A. P.; Xie, Y. L.; Lu, J. Q.; Luo, M. F. Enhanced activity for CO oxidation for Pr- and Cu-doped CeO_2 catalysts: Effect of oxygen vacancies. *J. Phys. Chem. C* **2008**, *112*, 15045−15051.
(17) Devaiah, D.; Tsuzuki, T.; Boningari, T.; Smirniotis, P. G.; Reddy, B. M. $Ce_{0.80}Mn_{0.08}O_{2-\delta}$ (M= Hf, Zr, Pr and La) ternary oxide solid solutions with superior properties for CO oxidation. *RSC Adv.* **2015**, *5*, 30275−30285.
(18) Liu, Z.; Liu, Y.; Chen, B.; Zhu, T.; Ma, L. Novel Fe-Ce-Ti catalyst with remarkable performance for the selective catalytic reduction of NO_x by NH_3. *Catal. Sci. Technol.* **2016**, *6*, 6688−6696.
(19) Tang, Y.; Zhang, H.; Cui, L.; Ouyang, C.; Shi, S.; Tang, W.; Li, H.; Lee, J.-S.; Chen, L. First principle investigation on redox properties of M-doped CeO_2 (M = Mn, Pr, Sn, Zr). *Phys. Rev.* **2010**, *82*, 125104.
(20) Westermann, A.; Geantet, C.; Vernoux, P.; Loridant, S. Defects band enhanced by resonance Raman effect in praseodymium doped CeO_2. *J. Raman Spectrosc.* **2016**, *47* (10), 1276−1279.
(21) Xu, J.; Long, K. Z.; Wu, F.; Xue, B.; Li, Y. X.; Cao, Y. Efficient synthesis of dimethyl carbonate via transesterification of ethylene carbonate over a new mesoporous ceria catalyst. *Appl. Catal., A* **2014**, *484*, 1−7.
(22) Huang, F.; Wang, S.; Zhang, S.; Fan, Y.; Li, C.; Wang, C.; Liu, C. Synthesis of Praseodymium-doped TiO_2 nanocatalysts by sol-microwave and their photocatalytic activity study. *Bull. Korean Chem. Soc.* **2014**, *35* (8), 2512−2518.
(23) Chen, Y.; Wang, H.; Qin, Z.; Tian, S.; Ye, Z.; Ye, L.; Abroshan, H.; Li, G. $Ti_xCe_{1-x}O_2$ Nanocomposites: A monolithic catalyst for direct conversion of carbon dioxide and methanol to dimethyl carbonate. *Green Chem.* **2019**, *21*, 4642−4649.
(24) Schwarz, J. A.; Contescu, C.; Contescu, A. Methods of preparation of catalytic materials. *Chem. Rev.* **1995**, *95*, 477−510.
(25) Huang, Y. Y.; Terentjev, E. M. Dispersion of carbon nanotubes: Mixing, sonication, stabilization and composite properties. *Polymers* **2012**, *4*, 275−295.
(26) Kesari, S.; Salke, N. P.; Patwe, S. J.; Achary, S. N.; Sinha, A. K.; Sastry, P. U.; Tyagi, A. K.; Rao, R. Structural stability and an harmonicity of $Pr_2Ti_2O_7$: Raman spectroscopic and XRD studies. *Inorg. Chem.* **2016**, *55*, 11791−11800.
(27) Ting, K. W.; Toyao, T.; Siddiki, S. M. A. H.; Shimizu, K.-i. Low-temperature hydrogenation of CO_2 to methanol over heterogeneous TiO_2-supported Re catalysts. *ACS Catal.* **2019**, *9*, 3685−3693.
(28) Makuch, E.; Wroblewska, A. Preparation of titanium-silicate Ti-SBA-15 catalyst. *Chemik* **2013**, *67* (9), 811−816.
(29) Tayade, R. J.; Kulkarni, R. G.; Jasra, R. V. Photocatalytic degradation of aqueous nitrobenzene by nanocrystalline TiO_2. *Ind. Eng. Chem. Res.* **2006**, *45*, 922−927.
(30) Fu, Z.; Zhong, Y.; Yu, Y.; Long, L.; Xiao, M.; Han, D.; Wang, S.; Meng, Y. TiO_2 Doped CeO_2 nanorod catalysts for direct conversion of CO_2 and CH_3OH to dimethyl carbonate: Catalytic performance and kinetic Study. *ACS Omega* **2018**, *3*, 198−2017.
(31) Liu, B.; Li, C.; Zhang, G.; Yao, X.; Chuang, S. S. C.; Li, Z. Oxygen vacancy promoting dimethyl carbonate synthesis from CO_2 and methanol over Zr-doped CeO_2 nanorods. *ACS Catal.* **2018**, *8*, 10446−10456.
(32) Majeed, S.; Shiva Shankar, S. A. Pr_6O_{11} micro-spherical nano-assemblies: Microwave- assisted synthesis, characterization and optical properties. *Mater. Chem. Phys.* **2013**, *143*, 155−160.
(33) Davydov, A. A.; Shepotko, M. L.; Budneva, A. A. Basic sites on the oxide surfaces: Their effect on the catalytic methane coupling. *Catal. Today* **1995**, *24*, 225−230.
(34) Wei, T.; Wang, M.; Wei, W.; Sun, Y.; Zhong, B. Effect of base strength and basicity on catalytic behavior of solid bases for synthesis of dimethyl carbonate from propylene carbonate and methanol. *Fuel Process. Technol.* **2003**, *83* (1−3), 175−182.
(35) De Filippis, P.; Scarsella, M.; Borgianni, C.; Pochetti, F. Production of dimethyl carbonate via alkyene carbonate tranesetrification catalyzed by basic salts. *Energy Fuels* **2006**, *20* (1), 17−20.
(36) Pyrlik, A.; Hoelderich, W. F.; Muller, K.; Arlt, W.; Strautmann, J.; Kruse, D. Dimethyl carbonate via transesterification of propylene carbonate with methanol over ion exchange resins. *Appl. Catal., B* **2012**, *125*, 486−491.
(37) Kumar, P.; Srivastava, V. C.; Mishra, I. M. Synthesis and characterization of Ce-La oxides for the formation of dimethyl carbonate by transesterification of propylene carbonate. *Catal. Commun.* **2015**, *60*, 27−31.
(38) Wang, Q.; Li, F.; Zhao, H-h; Kuang, Z-q; Wang, F.; Li, L.; Zhao, N.; Xiao, F-k Preparation of Mg-Al solid base for the transesterification of propylene carbonate and methanol. *J. Fuel Chem. Technol.* **2020**, *48* (4), 448−455.

https://doi.org/10.1021/acs.energyfuels.2c02235
Energy Fuels 2022, 36, 13148−13158